NRIAG JOURNAL OF ASTRONOMY AND GEOPHYSICS
2020, VOL. 9, NO. 1, 499–511
https://doi.org/10.1080/20909977.2020.1784697

Estimation of seismic site effect at the new Tiba City proposed extension, Luxor, Egypt

Abdelnasser Mohamed[a], Sayed Mohamed Ali[a] and Alaa Mostafa[b]

[a]Seismology Department, National Research Institute of Astronomy and Geophysics (NRIAG), Helwan, Cairo, Egypt; [b]Geology Department, Faculty of Sciences, Al-Azhar University, Assiut, Egypt

ABSTRACT
The Horizontal-to-Vertical Spectral Ratio (HVSR) technique is one of the most suitable tools for estimating the geological effect on ground motion. The main target of this study is to estimate the site effect and the fragility index value at the new Tiba City proposed extension. To achieve these targets, 21 ambient vibration recordings were conducted with 1 km grid to cover the investigated area. The estimated predominant frequency (f_0) distribution is a relative uniform and occurs at low frequency, ranging from 0.35 to 0.75 Hz and its maximum corresponding amplitude of seismic wave (A_0) starts from 3.1 up to 6.5. The qualitative interpretation of loose sedimentary cover thickness is large (136 to 410 m with average ~270 m) that coincided with occurrence of (f_0) at low level. The fragility index for the ground (K_g) at each measured site was computed depending on the estimated H/V amplitude and corresponding (f_0), and found to range from 17 to 118 across the investigated area. The highest values of K_g were obviously found in the northeastern part of the proposed site, where the highest amplification factor and the lowest fundamental frequency are found.

ARTICLE HISTORY
Received 13 April 2020
Revised 29 May 2020
Accepted 15 June 2020

KEYWORDS
Tiba City; HVSR method; fundamental frequency; amplification; fragility index

1. Introduction

cConstruction of new urban areas in desert regions became one of the main national targets for establishment of new communities. Due to the rapid increasing of the population, Egypt started to construct many development projects including new urban areas to face this increasing. Construction of such new urban areas especially in south Egypt will add to the new developed projects according to the Egyptian government's sustainable development plane. New Tiba City is one of these innovative communities. The proposed site of this city is placed east of the Nile River, 14 km northeast of Luxor city, the gate of the ancient civilisation (Figure 1). New Tiba City was constructed according to the government decision in 2000, and according to the sustainable development plan to complete all the development projects in this region, Egypt decided to extend the area of the city. The proposed extension site is located in an area surrounding by the main effective seismic regions in south Egypt (e.g. Aswan, the epicentre of 1981 earthquake with magnitude 5.6 and the Red Sea where Abu Dabbab area the source of 1955 (M = 5.6) and 1984 (M = 5.1) earthquakes). As a consequence of the importance of the area, it is become of prime interest to perform such study in the planning stage. The area is situated between latitude 25.71178° and 28.78008°N and longitudes 32.79512° and 32.80089°E (Figure 1). This area is connected with Aswan–Cairo highway by asphaltic road at about 10 Km from Luxor and also is connected with Luxor airport by another asphaltic road parallel to Aswan–Cairo highway. The proposed extension of new Tiba City covers a surface area of about 17 Km^2.

This work aims to estimate the site effect in terms of (f_0), the associated amplification (A_0) and the liquefaction potentiality by calculating the K_g using the HVSR technique. The most significant factor for the site effect is the soil condition. The site amplification exists when the seismic waves pass near the surface through soft soil layer and their amplitude increase significantly due to the impedance contrast between the soft and the bedrock layers. This phenomenon is a main factor influencing the extent of damage on structures (Safak 2001). The site effect has become an important factor for seismic hazard assessments and risk reduction programmes, so the output of HVSR measurements should be taken into consideration for building design and zoning purposes by decision-makers. Many studies (e.g. Field and Jacob 1993; Ohmachi et al. 1994; Ibs-von Seht and Wohlenberg 1999; Delgado et al. 2000; Parolai et al. 2002) demonstrated that the frequency at which the maximum amplitude of the H/V occurs is a good estimate for site resonance frequency, which can be attributed to the soft sediments thickness through an empirical relationship. Many researches have been proved that K_g-

CONTACT Abdelnasser Mohamed nassermhmd@yahoo.com National Research Institute of Astronomy and Geophysics (NRIAG), Helwan, Cairo, Egypt

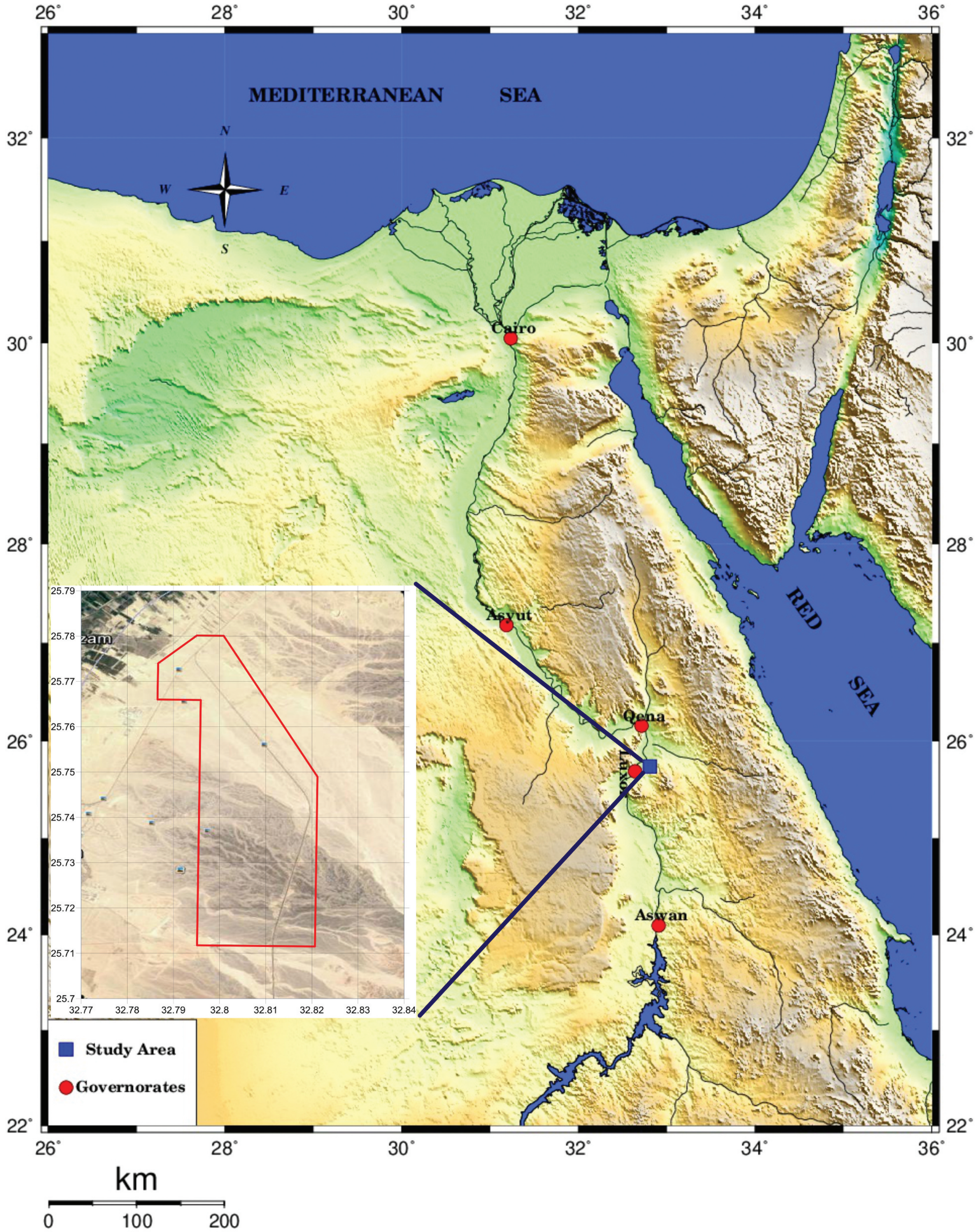

Figure 1. Location map of the study area.

value is high where the damage risk caused by earthquakes is high (Nakamura 1996, 1997, 2000). Since this approach is possible to be performed before earthquake occurrence, these measurements represent useful parameters for earthquake hazard assessment and damage mitigation. Different studies have been conducted in southern part of Egypt to estimate the site effect using the HVSR technique (e.g. Mohamed 2010; Mohamed and Fat-Helbary 2010; Mohamed et al. 2013, 2015).

2. Geological setting

The proposed site is located east of the Nile in Luxor area. The Quaternary deposits cover the surface of the area in

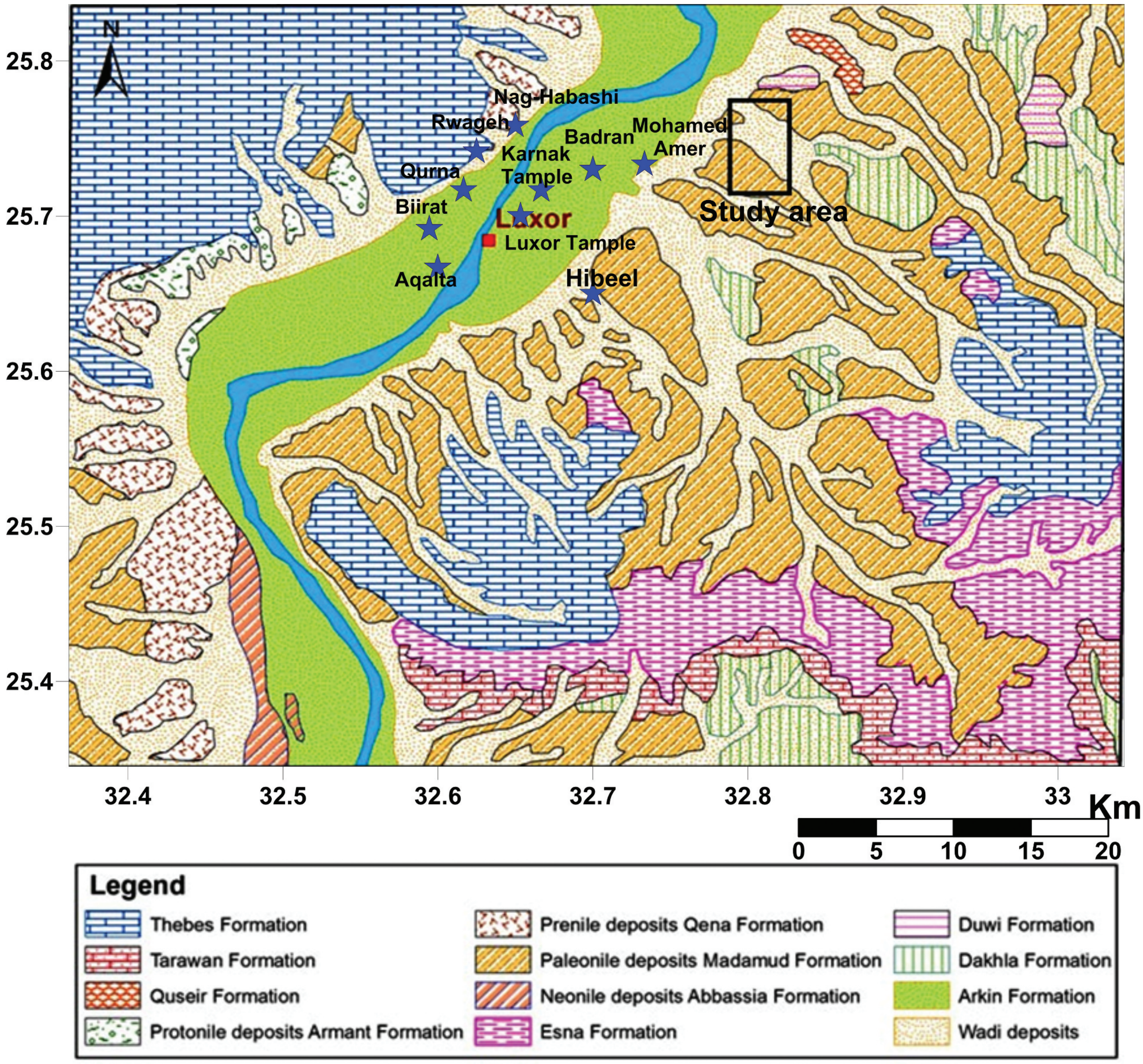

Figure 2. Geological map of Luxor area (Ayman 2009).

the form of loose sediments composed mainly of alluvial sands, gravel, clay or silt and Wadi deposits. Geologically, Luxor area (Figure 2) represents by Upper Cretaceous, Palaeocene–Eocene, Pliocene, and Pleistocene–Holocene (Said 1981; Kamel 2004) as follows: The Pliocene unit comprises the sediments of the Paleonile river system. In the eastern side, it is represented by Madamud Formation, which consists of interbedded red brown clays with thin fine-grained sand and silt lamina.

The subsurface stratigraphic sequence of Luxor area is shown in (Figures 3 & 4), where the data of ten wells have been collected and sited herewith. Eight wells from them are relatively deep down to more than 85 m (three wells were drilled in the eastern side, while other five wells were drilled in the western bank of Nile River, Luxor area). Three subsurface geochronologic units arranged from the bottom to top were previously recognised in the Luxor area (Said 1981), these are Pliocene unit, Pleistocene unit and Holocene unit. From correlation charts (Figures 3 & 4), the following can be delineated:

West of the Nile River: The subsurface sediments are essentially represented by silty clay, clay and clayey silt sediments that represent the cultivated region through the area. This unit is underlain by water-bearing sand, pebbly and boulder gravel, which represents Pleistocene aquifer in this area.

In the east of Nile River: The subsurface sediments are essentially represented by silty clay, clay, clayey silt and fine sand that represent the cultivated land through the area. This unit is underlain by water-bearing unit that consists of medium to coarse grain sand and gravel, which represents Pleistocene aquifer in the area.

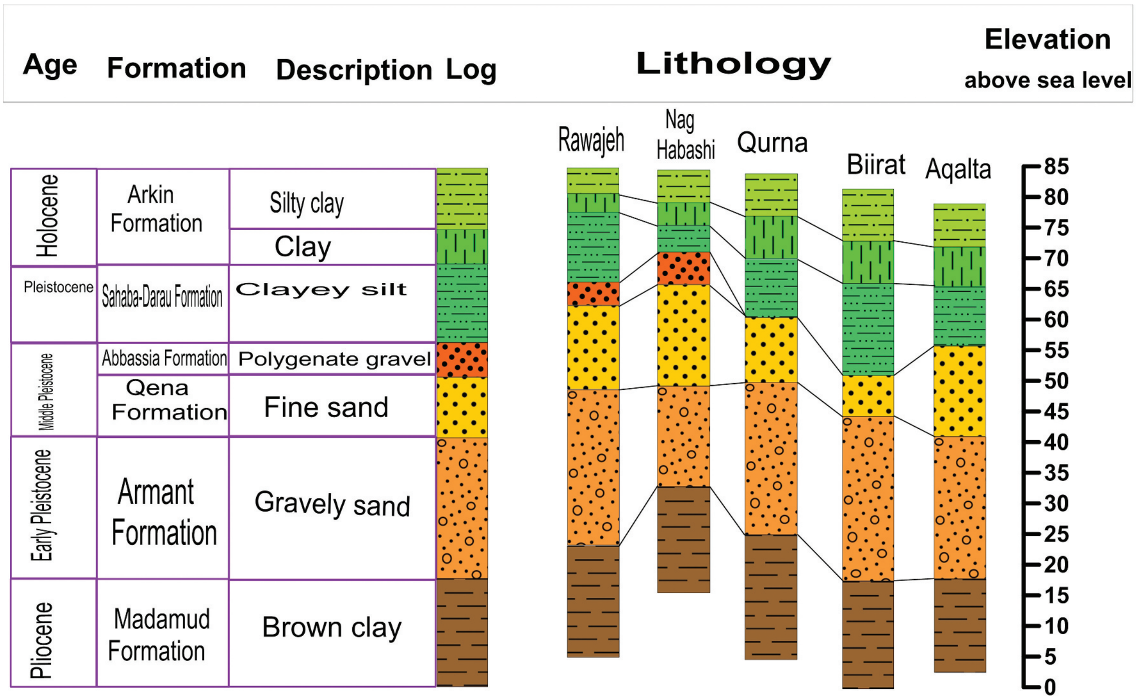

Figure 3. Lithostratigraphic correlation between five well from western bank of Luxor area showing vertical facies change from Pliocene – Holocene Formations (after Kamel 2004).

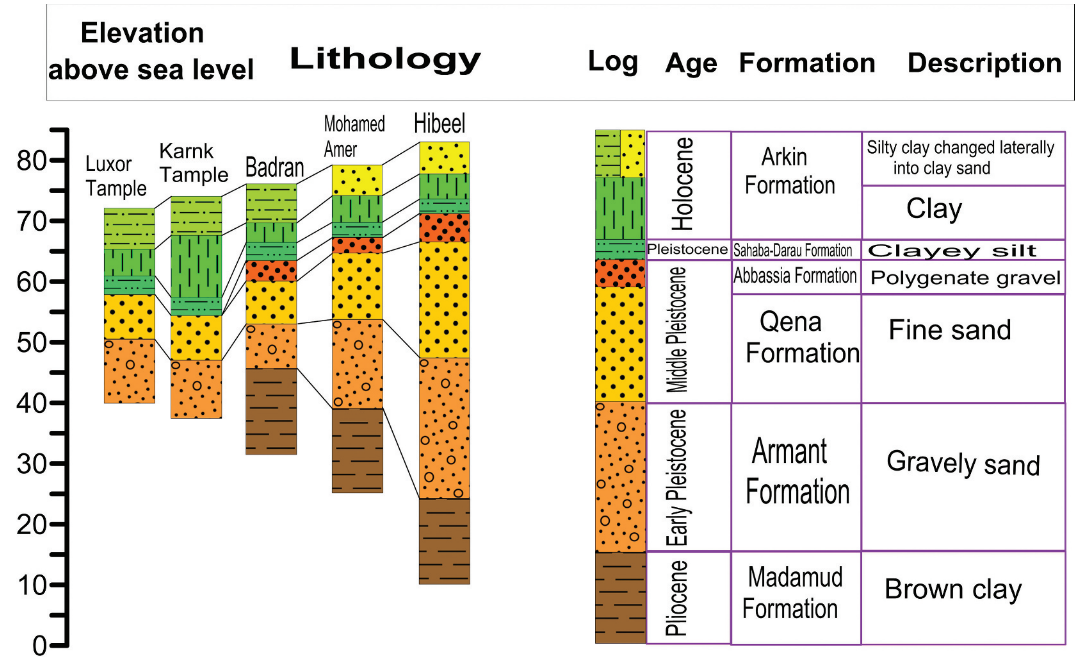

Figure 4. Lithostratigraphic correlation between idealised logs from Luxor and Karnak temples and three wells from three different location representing subsurface Pliocene – Holocene Formations of eastern bank of Luxor area (after Kamel 2004).

Figure 5. Typical geological structure of sedimentary basin (after Nakamura 2000).

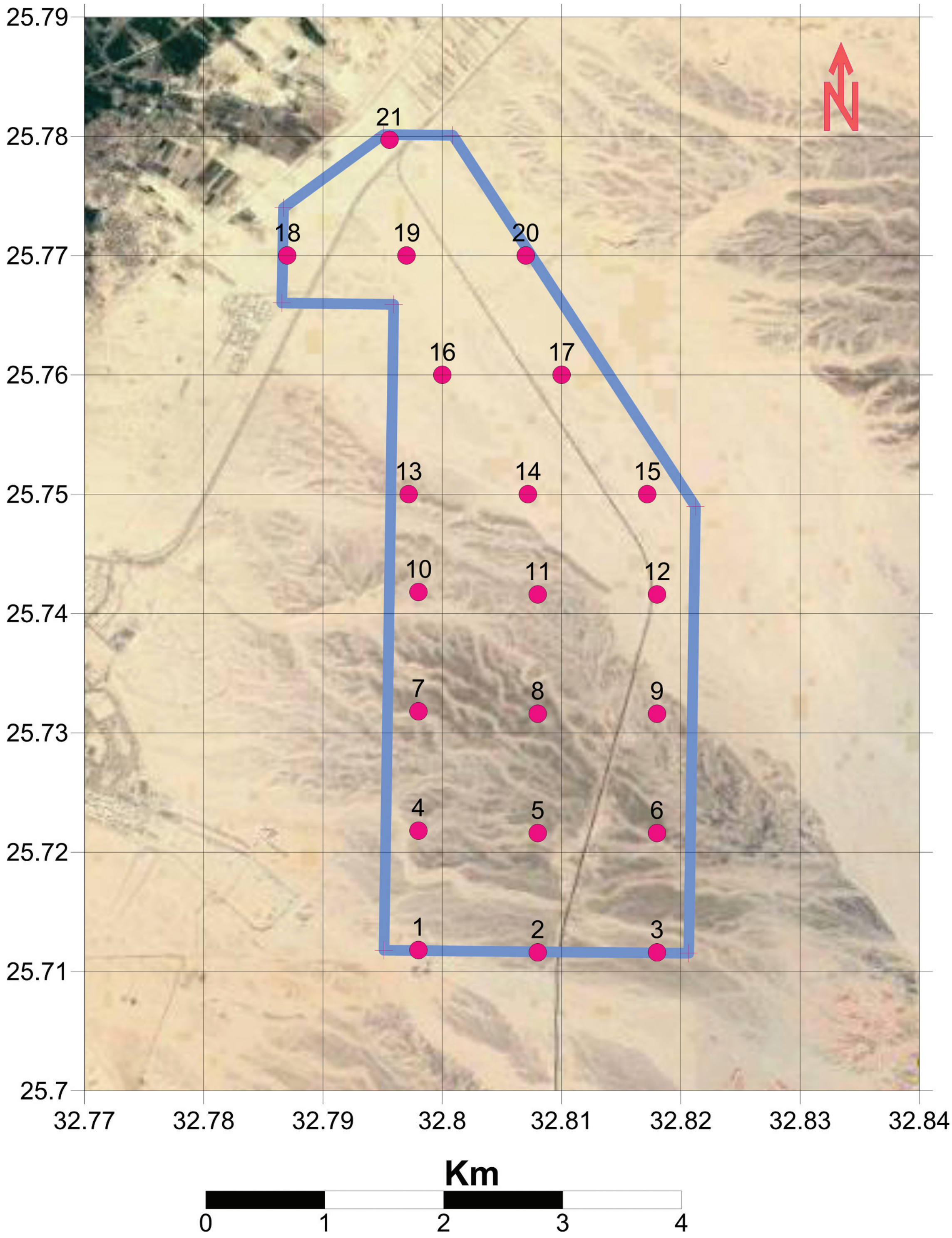

Figure 6. Location map of the microtremor measurements at the study area (the red circles are the measured points).

3. Methodology

3.1. HVSR method (Nakamura technique)

The HVSR technique is used to estimate the Fourier amplitude spectral ratio between the horizontal and vertical components of microtremors. This technique using microtremors recordings from a three-component portable station is one widely applicable technique for estimating local site effects. Nogoshi and Igarashi (1970, 1971) discussed the origin of the microtremor is derived from body waves or surface waves (Nakamura 2019), so the root of the method does not come from these studies, it comes from Nakamura (1989) when he debated its capability to estimate the resonance frequency of sedimentary cover. The HVSR method is the most applicable technique for estimation the soft sedimentary cover thickness

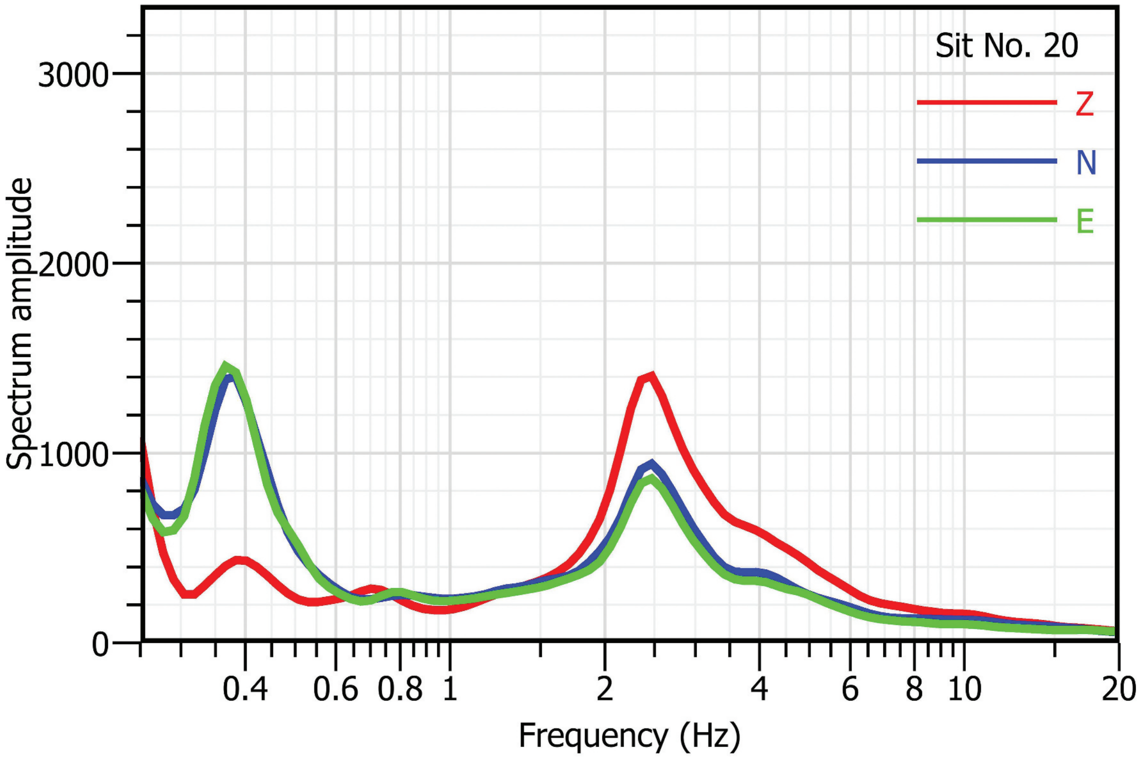

Figure 7. The amplitude spectrum of the three components at site No. 20 as a representative example in this study.

(e.g. Ibs-von Seht and Wohlenberg 1999; Parolai et al. 2002; Fäh et al. 2003; Hinzen et al. 2004; Toni et al. 2016a, 2016b; Trevisani et al. 2017; Trevisani and Boaga 2018; Abd El-aal 2018). The basic concept of Nakamura's technique can be described in a simplest case (Figure 5), in a one-dimensional soft sedimentary layer (soil: denoted as subscript "s") above bedrock (denoted as subscript "b"). In this case, the Fourier amplitude spectrum of the horizontal components on the surface layer is H_s and at the bedrock layer is H_b. The response of sediments can be given by the spectral ratio of the recorded signal on the surface to recorded signal on the bedrock.

The spectral ratio on the horizontal components as H_f can be expressed as

$$H_{\mathbf{f}} = H_{\mathbf{s}}/H_{\mathbf{b}} \tag{1}$$

And for the vertical components, V_f as

$$V_{\mathbf{f}} = V_{\mathbf{s}}/V_{\mathbf{b}} \tag{2}$$

where Vs and Vb are the spectra of the vertical component as recorded on sediments surface and bedrock. Nakamura (1989) proposed a "transfer function" S_t and expressed it as:

$$S_{\mathbf{t}} = H_f/V_{\mathbf{f}} \tag{3}$$

Substituting (1) and (2) in Equation (3) we get:

$$S_{\mathbf{t}} = (H_{\mathbf{s}}/H_{\mathbf{b}})/(V_{\mathbf{s}}/V_{\mathbf{b}}) = (H_{\mathbf{s}}/H_{\mathbf{b}}).(V_b/V_s) \tag{4}$$

$$S_{\mathbf{t}} = (H_{\mathbf{s}}/V_{\mathbf{s}}).(V_{\mathbf{b}}/H_{\mathbf{b}}) \tag{5}$$

And finally, by assuming that the ratio H_b/V_b is equal to unity, the site effect function, corrected by the source term, may be written as:

$$S_{\mathbf{t}} = (H_{\mathbf{s}}/V_{\mathbf{s}}) \tag{6}$$

3.2. Fragility (vulnerability) index for ground (K_g)

One of the simplest physical parameter that could be used to the site characteristics is the fragility index for the ground (K_g). It can be considered as an indicator which might be useful in selecting weak points of ground along the studied area. By using the HVSR, the site resonance frequency (f_0) and peak amplitude (A_0) were estimated. According to Nakamura (2019), the K_g value was used for risk evaluation of soil liquefaction depending on the results of (Nakamura and Takizawa 1990b) HVSR microtremors. Nakamura (1996, 1997) confirmed the correlation of the (K_g) value with soil liquefaction and also with damage to small buildings. The liquefaction of soil is a process by which sediments below water table tentatively lose shear strength and behave more like a viscous liquid than as a solid.

The K_g-value for the ground is simply derived from strains of ground (Nakamura 1996, 1997, 2000). It can be defined as:

$$K_g = A^2{}_{\mathbf{0}}/F_{\mathbf{0}} \tag{7}$$

where A_0 and F_0 are peak amplification factor and its predominant frequency, respectively, estimated by the HVSR technique. In this study, site characteristics at the studied area were conducted based on the HVSR and the

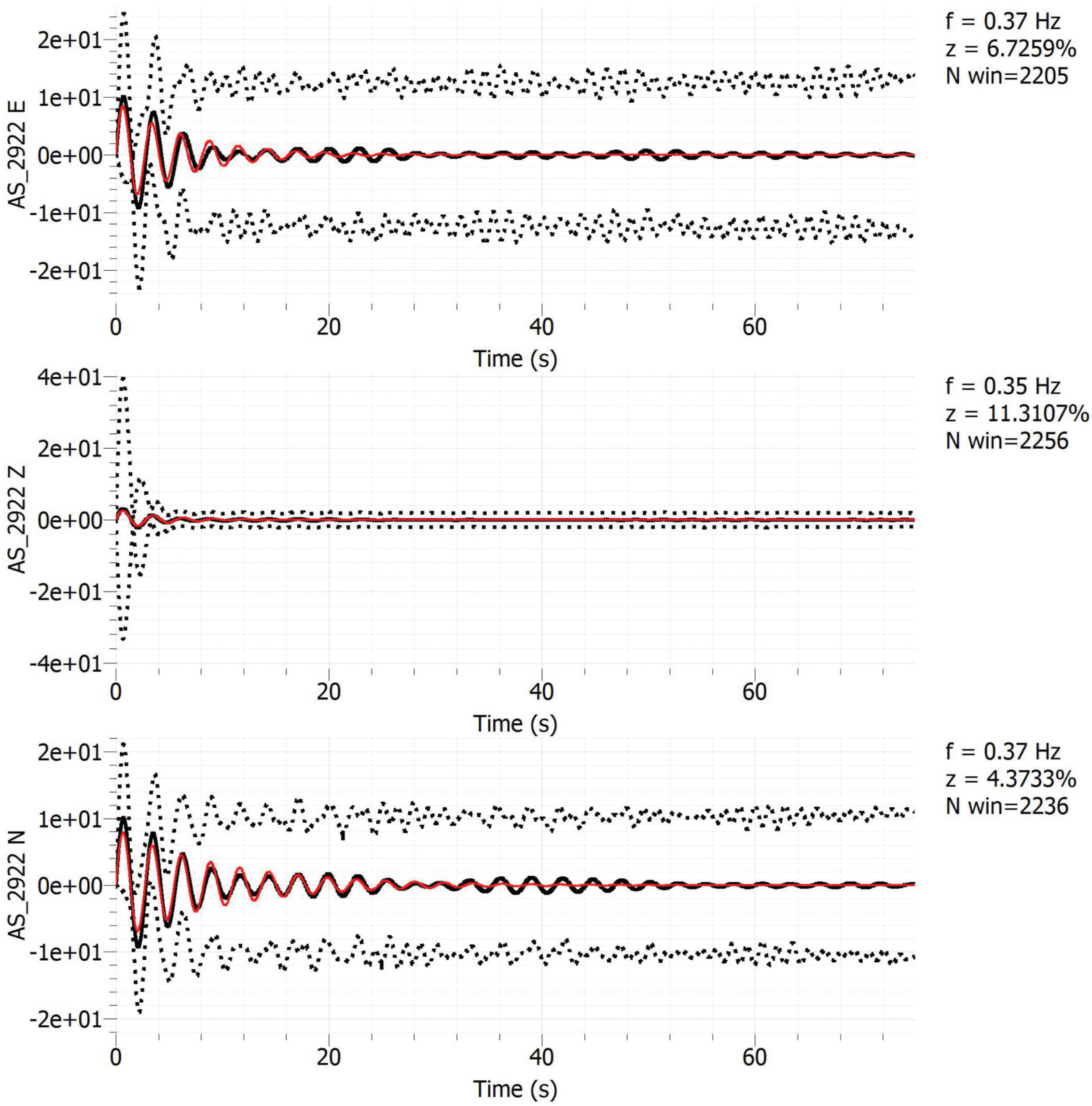

Figure 8. An example of the damping test for the peak amplitude at frequency 0.37 Hz of natural origin.

K_g-values to predict the risk of soil liquefaction. The application of this technique (i.e. determination of K_g from microtremor HVSR) has been recently applied in Egypt by Fergany and Omar (2017) and Meneisy et al. (2020) with reasonable results.

4. Data acquisition and analysis

4.1. Field survey

To have a good coverage over a whole of the study area, 21 microtremor measurements were planned on selected and well-distributed sites in a roughly about 1 km due to environmental constraints (Figure 6). The data were collected during the day time using three-component seismometer (Trillium compact 120 s) and a Taurus portable recorder. Continuous ambient vibration signals were recorded for 120 to 180 minutes duration at selected sites with a sample rate 100 sample/second for all sites following the guidelines of Nakamura (1996) and SESAME project (2004).

4.1. Data analysis

To describe the collected data and extract information, an extensive work on processing is necessary. The HVSR Nakamura's technique (1989) was used to analyse the microtremors recorded signals. The analysis was accomplished using Geopsy software (http://www.geopsy.org) that initiated with the European project (SESAME 2004). Data analysis was concentrated on frequency from 0.2 to 20 Hz which interesting for engineering applications. Each time window was selected using the automatic window selection option of the Geopsy software according to the principle of STA/LTA antitriggering, which detects transients with the goal of avoiding them in order to the selected signal contain only real seismic ambient vibrations (SESAME 2004; Wathelet

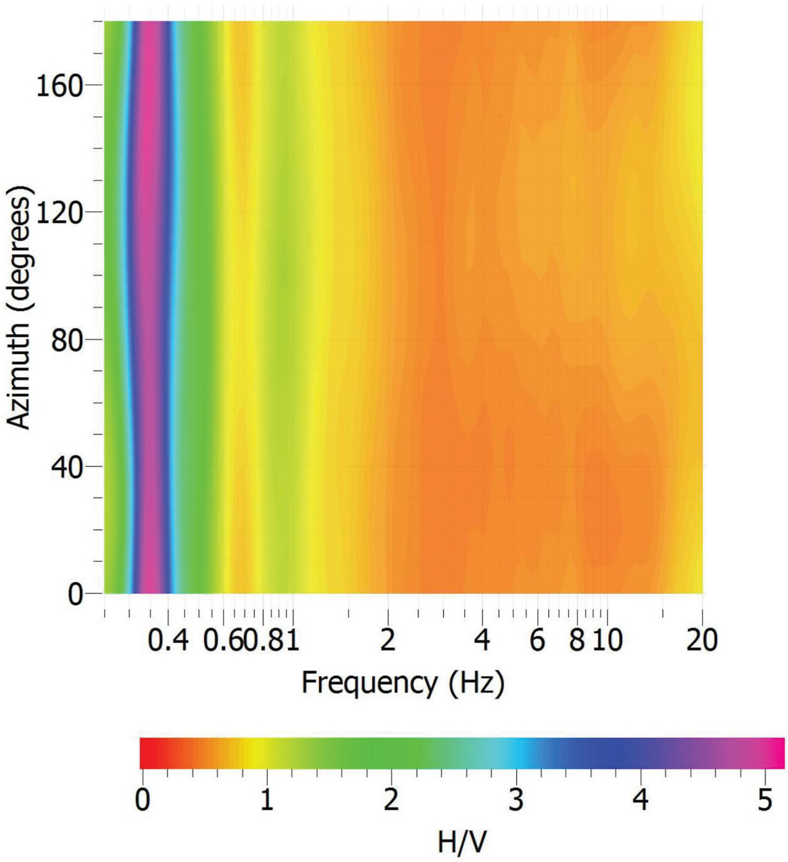

Figure 9. An example of the H/V rotation for 0.37 Hz frequency of natural origin.

2010). The recorded signal was subdivided into time windows with 75 second duration and at least 15 windows were used. Cosine tapering of the time series with 8% and smoothing of the Fourier amplitude spectra by the algorithm of Konno and Ohmachi (1998) with smoothing constant value 40 applied in the current data processing. Figure 7 illustrates the amplitude spectrum of the three components at site No. 20 as a representative example in this study. The peak that's may be have an industrial origin was checked by applying these tests:

(1) The random decrement technique (Dunand et al. 2002) was applied to the microtremors data to conclude the "impulse response" around the frequency of interest: if the corresponding damping (z) is very low (<1%), an industrial origin may be presented almost certainly, so the frequency should not be used in the interpretation (Figure 8).
(2) Applying the spectrum rotation for the horizontal components. This tool is useful to check the direction of energy release. Both rotated spectra and H/V curves were carried for all the measured sites (Figure 9).

After applying the required checks on all the recorded data, all appeared peaks found to be of natural source with damping value above 1%.

5. Results and interpretations

The dominant frequency and corresponding peak amplitude at 21 measured sites have been estimated over the targeted area (Table 1). In the case of a single peak (Figure 10), the corresponding frequency was interpreted as the resonance frequency (f_0). Few sites showed two/multi peaks at different frequencies (Figure 11), where the first one was interpreted as fundamental frequency and second peak can be attributed to shallow structure or presence of shallow bedrock with small impedance

Table 1. The output results in the study area.

Site No.	F_0(Hz)	A_0	K_g	Thickness (m)
1	0.35	4.7	62.8	409.7
2	0.42	4.9	58.9	321.6
3	0.51	4.1	33.9	241.7
4	0.40	5.5	75.4	343.6
5	0.43	5.5	69.8	302.0
6	0.75	3.9	19.9	136.1
7	0.51	4.2	34.5	236.5
8	0.70	4.1	23.7	150.5
9	0.70	6.4	58.5	151.0
10	0.60	4.1	27.4	187.9
11	0.59	3.9	26.0	195.3
12	0.59	3.1	16.8	194.0
13	0.57	3.8	25.2	205.6
14	0.60	3.5	19.9	187.7
15	0.57	3.6	22.7	203.3
16	0.50	4.5	40.4	246.8
17	0.48	3.9	32.1	258.5
18	0.48	3.6	26.5	262.5
19	0.40	3.9	37.4	342.3
20	0.36	6.5	117.8	398.2
21	0.35	4.9	67.6	405.9

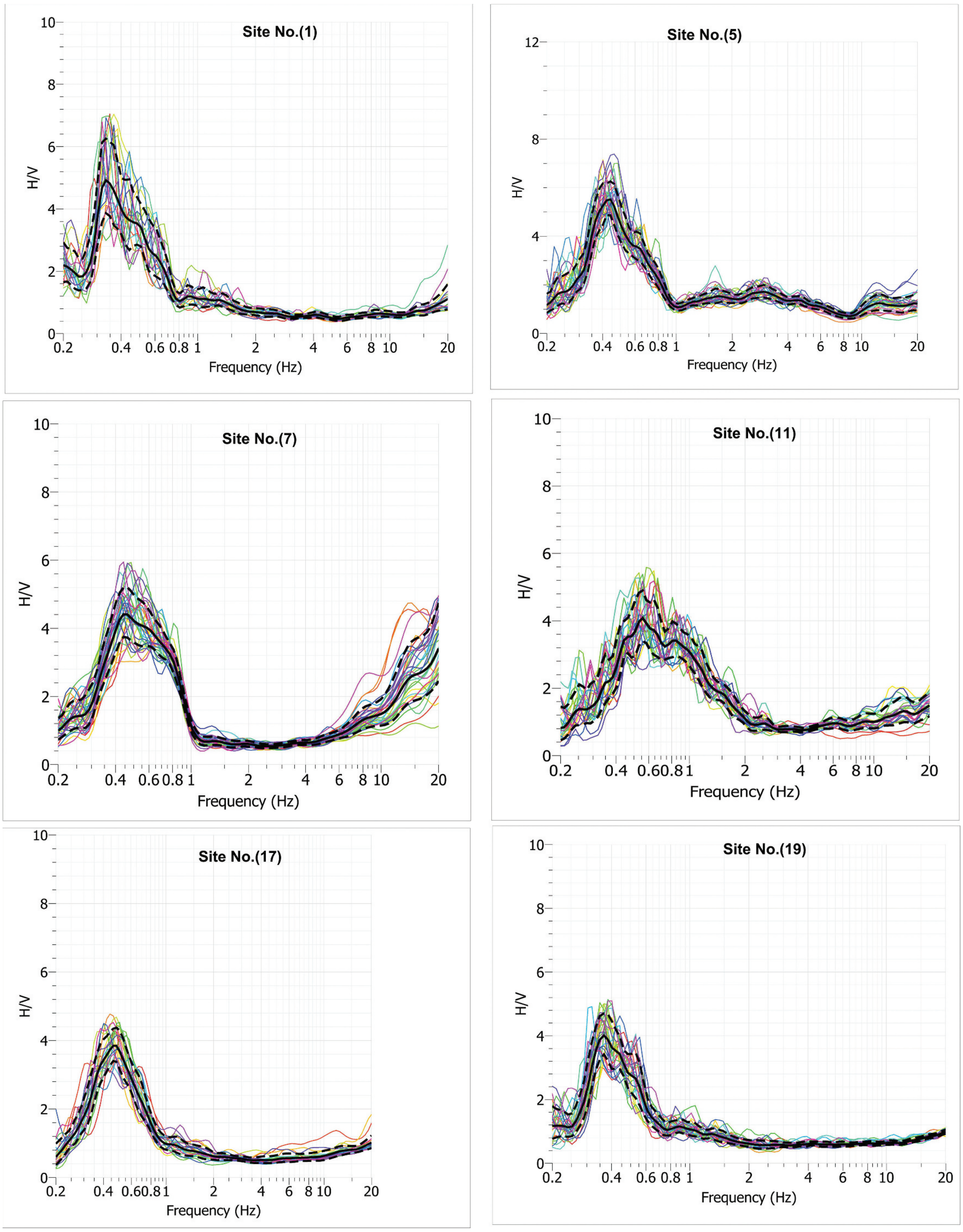

Figure 10. Examples of the H/V curves at the study area with a single clear peak at various frequencies, the output is a graph where the frequency is represented along the x-axis in logarithmic scale, the H/V ratio is along the y-axis in linear scale, and the selected coloured time windows are represented as corresponding coloured lines in the H/V plot from 0.2 to 20 Hz. The average H/V ratio and standard deviations were shown as the solid black line and the dotted black lines, respectively, while the peak of fundamental frequency was given by the grey column.

contrast between it and surface sediments. The zonation maps for the resonance frequency and the H/V amplitude were produced, as shown in Figures 12 and 13, respectively. The frequency (f_0) values for the proposed site (Figure 12) are varying from 0.35 to 0.75 Hz. Most of the lower frequencies ($f_0 < 0.5$ Hz) are found in the northern and southern parts of the investigated area where the alluvial plain zone mainly covered by a thick layer of Quaternary and Pliocene unconsolidated deposits area found, while the middle part area has frequencies (f_0) from 0.5 to 0.74 Hz. The H/V peak amplitude (A_0) has a value from 3.1 to 6.5 (Figure 13), where the northern and the southern parts are amplifying the ground motion more than the middle part. The site amplification level has been controlled by impedance contrast between the soft sedimentary cover and the bedrock layer, where the areas with higher amplification value having sharp impedance contrasts in the soil. The

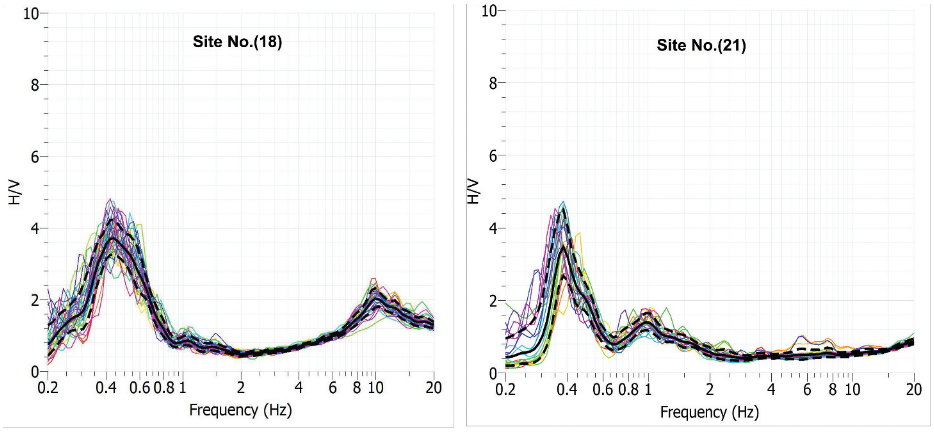

Figure 11. The same as in Figure 10 but with two clear peaks at various frequencies.

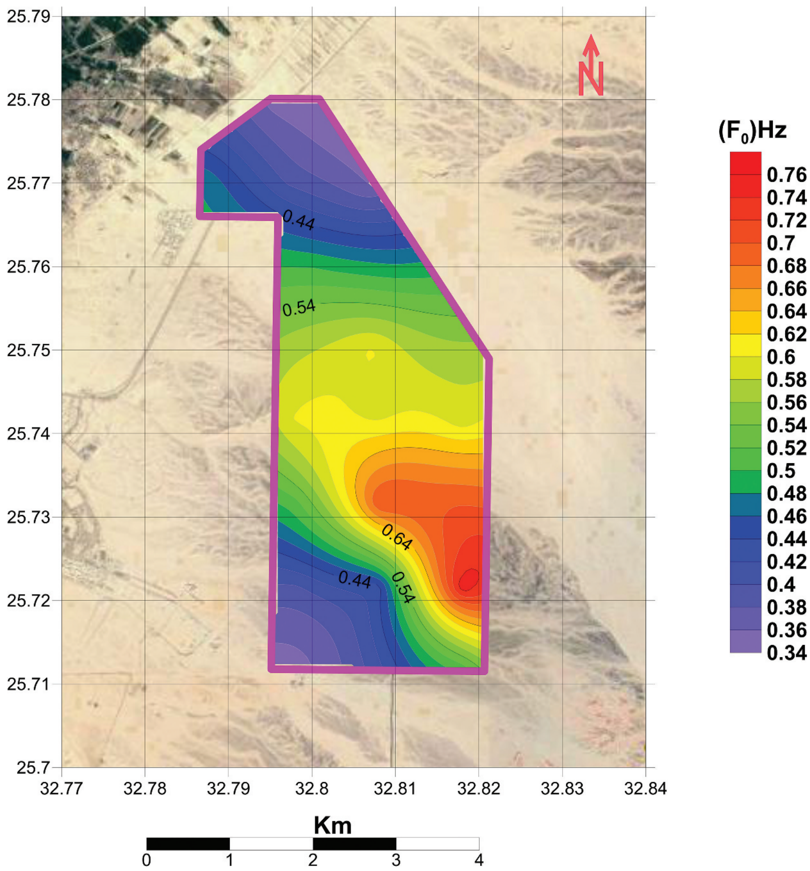

Figure 12. The fundamental frequency (f_0) distribution at the study area.

distribution of K_g-values in the proposed site is listed in Table 1 and Figure 14 is varying from 17 to 118. In general, the high values correspond to the high amplification in the northeastern part, while the low (K_g) locates in the centre of the area. In general, the variation of the K_g obtained from this study correlates well with the peak amplitude of the H/V curve, where the sites having large peak amplitude, the (K_g) is high and this is in a good correlation with field survey and wells lithology where the sedimentary cover in this area is mainly composed of silty clay, fine sand and gravely sand. Many authors (e.g. Ibs-von Seht and Wohlenberg 1999; Parolai et al. 2002; Abd El-aal 2018) discussed the estimation of the sedimentary thickness over the seismic bedrock based on seismic noise data (Nakamura technique). In our study, the derived equation of Abd El-aal (2018) was applied due to its consistency with the geological successions for different parts in Egypt. The calculated sedimentary thickness (Table 1) is ranging from 136 to 410 metre over the study area.

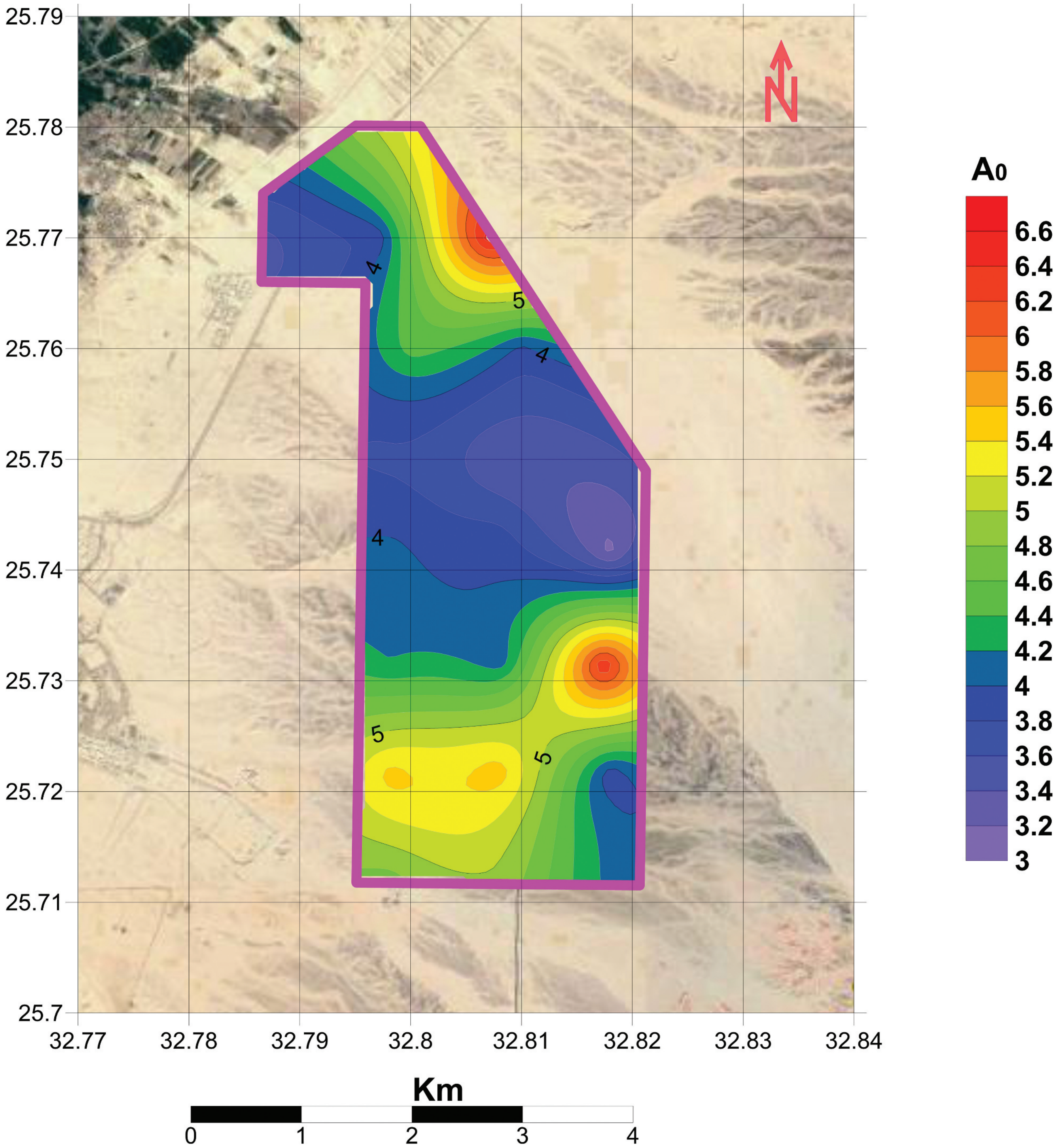

Figure 13. The H/V amplitude level (A_0) distribution at the study area.

6. Conclusion

The HVSR method (Nakamura's technique) has become one of the most easiest and inexpensive methods to understand the characteristics of subsurface layers. Twenty-one microtremor records were collected in the area, and the frequency (f_0), the peak amplitude (A_0) and the fragility index for the ground (K_g) were computed for site effect estimation.

In this study, the majority of the HVSR have a clear single peak; the interpretations for the HVSR results are obvious because the spectral ratio which has only one clear peak is interpreted to be the predominant frequency. In other cases clear two peaks were observed, the first one is the resonance frequency and the second one is certainly associated with a very shallow structure or due to the impedance contrast. The distribution of predominant frequency is ranging from 0.35 to 0.75 Hz; these low-frequency values reflect to the soft sediments with large thickness. The H/V peak amplitude has values between 3.1 and 6.5. The fragility index for the ground (K_g) was estimated to identify the areas where degree of earthquake hazards and damage may be expected using the HVSR technique. The calculated K_g is ranging from 17 to 118, the large values concentrated in northern and southern parts of the area where the field observations indicated that areas have a water table less than

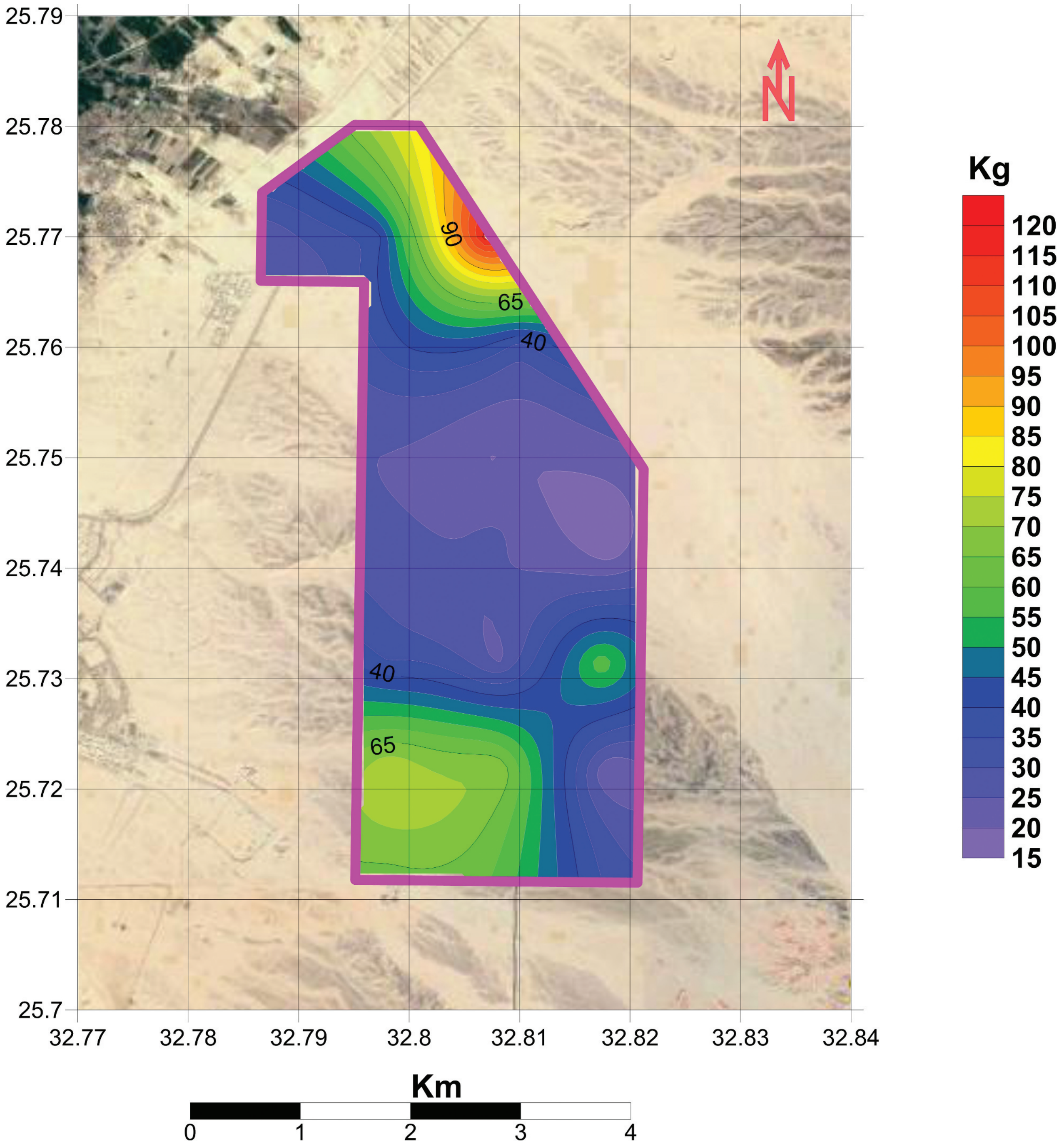

Figure 14. The seismic vulnerability index (Kg) distribution at the study area.

20 m depth. The high K_g values indicate that the area has high potential for damage and deformation due to liquefaction during earthquake occurrence. Overall results reflect low values of the frequency (f_0) and corresponding greater values of the K_g, thus indicating a greater seismic risk elicited by soil amplification in the area under investigation. By applying the HVSR method in this study, the site effect (f_0 & A_0) and the K_g were estimated in the study area. The output results showed different zoning maps illustrated the high-risk areas which will affect strongly during the earthquake occurrence.

Acknowledgements

Authors are thankful to Aswan Earthquake Research Center (National Research Institute of Astronomy and Geophysics (NRIAG)), for providing us with the seismic instruments data used in this research. Our indebted gratitude goes to our colleagues from our organizations, who have contributed somehow, whether in data collection, sharing, or discussion methods concerning this study.

Disclosure statement

No potential conflict of interest was reported by the authors.

References

Abd El-aal AK. 2018. New relationship between fundamental site frequency and thickness of soft sediments from seismic ambient noise. J Seismol. 22:1315–1323. doi:10.1007/s10950-018-9753-x.

Ayman A. 2009. Land use change and deterioration of pharaonic monuments in upper Egypt. J Eng Sci Assiut Univ. 37(1):161–177.

Delgado J, Lopez Casado C, Giner J, Este´vez A, Cuenca A, Molinal S. 2000. Microtremors as a geophysical exploration tool: applications and limitations. Pure Appl Geophys. 157:1445–1462. doi:10.1007/PL00001128.

Dunand F, Bard P, Chatelain J, Guéguen P, Vassail T, Farsi M. 2002. Damping and frequency from Randomdec method applied to in situ measurements of ambient vibrations. Evidence for effective soil structure interaction. 12th European Conference on Earthquake Engineering; London. p. 869.

Fäh D, Kind F, Giardini D. 2003. Inversion of local S-wave velocity structures from average H/V ratios, and their use for the estimation of site-effects. J Seismol. 7(4):449–467. doi:10.1023/B:JOSE.0000005712.86058.42.

Fergany E, Omar K. 2017. Liquefaction potential of Nile delta, Egypt. NRIAG J Astron Geophys. 6(1):60–67. doi:10.1016/j.nrjag.2017.01.004.

Field EH, Jacob K. 1993. The theoretical response of sedimentary layers to ambient seismic noise. Geophys Res Lett. 20:2925–2928. doi:10.1029/93GL03054.

Hinzen KG, Weber B, Scherbaum F. 2004. On the resolution of H/V measurements to determine sediment thickness, a case study across a normal fault in the Lower Rhine Embayment, Germany. J Earthquake Eng. 8(6):909–926. doi:10.1080/13632460409350514.

Ibs-von Seht M, Wohlenberg J. 1999. Microtremor measurements used to map thickness of soft sediments. Bull Seism Soc Am. 89:250–259.

Kamel ER. 2004. Geology of Luxor area and its relationship to groundwater uprising under the pharaohs temples [M. Sc. Thesis]. Egypt: Aswan Faculty of Science, South Valley University.

Konno K, Ohmachi T. 1998. Ground-motion characteristics estimated from spectral ratio between horizontal and vertical components of microtremor. Bull Seism Soc Am. 88(1):228–241.

Meneisy AM, Toni M, Omran AA. 2020. Soft sediment characterization using seismic techniques at Beni Suef city, Egypt. Environ Eng Geophys. (in press).

Mohamed A. 2010. Engineering seismology studies for land use planning at the proposed Tushka New City site, South Egypt [PhD Thesis]. Aswan University.

Mohamed A, Fat-Helbary R. 2010. Microtremors measurements for site effect investigation at Aswan New City, Egypt. The Proceedings of the 14th European Conference of Earthquake Engineering (14ECEE); 30 August-03 September; Macedonia.

Mohamed A, Fat-Helbary R, Basheer AA, Dojcinovski D. 2013. Using ambient vibrations for site characterization at the new Aswan University site, southern Egypt. SE50EEE International Conference on Earthquake Engineering; May 29–31; Macedonia.

Mohamed A, Lindholm C, Girgis M. 2015. Site characterization and seismic site response study of the Sahary area, South Egypt. Acta Geodyn Geomater. 12(4 (180)):427–436. doi:10.13168/AGG.2015.0032.

Nakamura Y. 1989. A method for dynamic characteristic estimation of subsurface using microtremors on the ground surface. Railway Tech Res Inst Q Rep. 30:25–33.

Nakamura Y. 1996. Real-time information systems for hazards mitigation. Proceedings of the Xth World Conference on Earthquake Engineering, Acapulco, # 2134; Elsevier.

Nakamura Y. 1997. Seismic vulnerability indices for ground and structures using microtremor. World Congress on Railway Research in Florence; Italy.

Nakamura Y. 2000. Clear identification of fundamental idea of Nakamura's technique and its applications. Auckland (New Zealand). 12WCEE, 2656.

Nakamura Y. 2019 July/August. What is the Nakamura method? Seismol Res Lett.90(4):1437–1443.

Nakamura Y, Takizawa T. 1990b. Prediction of liquefaction using microtremor. Proceeding of the 45th Annual Meeting of JSCE, I-519. p. 1068–1069. (in Japanese).

Nogoshi M, Igarashi T. 1970. On the propagation characteristics estimations of subsurface using microtremors on the ground surface. J Seism Soc Jpn. 23:264–280.

Nogoshi M, Igarashi T. 1971. On the amplitude characteristics of microtremor (part 2). J Seismol Soc Jpn. 24: 26–40. (in Japanese with English abstract).

Ohmachi T, Konno K, Endoh T, Toshinawa T. 1994. Refinement and application of an estimation procedure for site natural periods using microtremor. J Jpn Soc Civ Eng. 489(1–27):251–261.

Parolai S, Bormann P, Milkereit C. 2002. New relationships between Vs, thickness of sediments, and resonance frequency calculated by the H/V ratio of seismic noise for the Cologne area (Germany). Bull Seismol Soc Am. 92:2521–2526. doi:10.1785/0120010248.

Safak E. 2001. Local site effects and dynamic soil behavior. Soil dynamics and earthquake engineering. 21:453–458.

Said R. 1981. The geological evolution of the Nile River. NewYork: Springer -Verlag; p. 151.

SESAME. 2004. Site effects assessment using ambient excitations: guidelines for the implementation of the H/V spectral ratio technique on ambient vibrations measurements, processing and interpretation. European research project, WP12.

Toni M, Abd El-aal AK, Mohamed GA. 2016a. Ambient noise for determination of site dynamic properties at Hurghada and Safaga cities, Red Sea, Egypt, Acta geodyn. Geomater. 13(3):227–240. doi:10.13168/AGG.2016.0004..

Toni M, Mohamed GA, Abd El-aal AK. 2016b. Microtremor for Evaluating the Effect of Shallow Sediments on Earthquake Ground Motion at Quseir City, Red Sea, Egypt. Near Surface Geoscience 2016-22nd European Meeting of Environmental and Engineering Geophysics; Sept 4–8; Barcelona, Spain.

Trevisani S, Boaga J. 2018. Passive seismic prospecting in venice historical center for impedance contrast mapping. Environ Earth Sci. 77(21):733. doi:10.1007/s12665-018-7918-0.

Trevisani S, Boaga J, Agostini L, Galgaro A. 2017. Insights into bedrock surface morphology using low-cost passive seismic surveys and integrated geostatistical analysis. Sci Total Environ. 578:186–202. doi:10.1016/j.scitotenv.2016.11.041.

Wathelet M. 2010. Geopsy project. http://www.geopsy.org/index.html